



FINAL PUBLISHABLE JRP REPORT

JRP-Contract number	IND55		
JRP short name	MClOCKs		
JRP full title	Compact and high-performing microwave clocks for industrial applications		
Version numbers of latest contracted Annex Ia and Annex Ib against which the assessment will be made	Annex Ia:	V1.0	
	Annex Ib:	V1.0	
Period covered (dates)	From	01 June 2013	To 31 May 2016
JRP-Coordinator			
Name, title, organisation	Salvatore Micalizio, Dr, INRIM		
Tel:	+390113919230		
Email:	s.micalizio@inrim.it		
JRP website address	http://www.inrim.it/Mclocks/		
Other JRP-Partners			
Short name, country	OBSPARIS, France TUBITAK, Turkey UFC, France Muquans, France		
REG-Researcher (associated Home Organisation)			
Researcher name, title (Home organisation Short name, country)	Gaetano Mileti, Prof Université de Neuchatel (Switzerland)	Start date: 01 August 2013 Duration: months 32	

Report Status: PU Public





TABLE OF CONTENTS

1	Executive Summary.....	3
2	Project context, rationale and objectives.....	4
3	Research results	5
3.1	Review of the microwave vapour-cell clocks (commercial and research devices).....	5
3.2	Development of a Pulsed Optically Pumped Rb frequency standard.....	6
3.2.1	Development of a prototype of POP Rb clock.....	6
3.2.2	Clock characterization.....	12
3.3	Development of an industry-ready frequency standard based on cold Rb atoms.....	15
3.3.1	Clock implementation.....	16
3.3.2	Clock characterization.....	19
3.4	CPT alternative approach.....	21
3.4.1	Clock implementation.....	21
3.4.2	Clock characterization.....	23
3.5	Resume of the results achieved in the Mclocks project.....	25
4	Actual and potential impact.....	26
5	Website address and contact details.....	27
6	List of publications.....	27



1 Executive Summary

Introduction

Atomic frequency standards provide the ultimate source of accuracy and stability for all modern communication, navigation and timekeeping systems. There is a demand from industry for more accurate and stable clocks. Several Rubidium (Rb) based prototype clocks with unprecedented frequency stability have been developed by specialised laboratories using laser sources and innovative techniques to prepare and detect the atoms. In this project, the prototypes are developed and improved to make them suitable for industrial use, commercial production and to transfer frequency standards between laboratories and from laboratories to clock manufacturers. Commercial clock manufacturers want clock technology which reproduces laboratory performance, but with portability, reliability and low power consumption.

The Problem

A wide range of scientific and technological fields requires stable and reliable frequency standards and timekeeping. Often only atomic clocks can provide these signals with the required level of accuracy and stability. There are three areas which need the development of compact clocks with high metrological features:

1. Technological applications where frequency stability is the main concern (of the order of 10^{-12} - 10^{-13} at 1s measurement time), for example, telecommunications, navigation, defence and space. Currently Rb clocks are used, and if the requirement for stability is particularly stringent Rb clocks are replaced by hydrogen masers (H-masers). However, they are bulky, very expensive and only a few laboratories or industries can afford them. The ideal would be a clock combining the performance of an H-maser with the low price, reliability and compactness of a Rb clock. This is required for the European satellite system GALILEO, which currently has on board a performing (but heavy) hydrogen maser and a lower performing Rb clock. Reducing the payload would bring financial benefits for each launch.
2. Applications where size is primary importance (for example a volume of the order of 20 cm^3 and a weight of 50 g). This is important when the clock operates inside measurement instruments, in vehicles or in unmanned devices. They are important role in military applications, especially in GPS-denied environment. In addition, the small size, jointly with a stability of some 10^{-12} (1 hour measurement time), opens the door to new classes of applications such as underwater sensors for seismic research or gas and oil exploration.
3. Advanced applications where stability, accuracy and reduced size, weight and cost are all highly desirable. This is the case in metrological laboratories. Currently, they use an H-maser to optimise the short-term performances and a master Cs clock to optimise the medium to long term behaviour. In addition, most advanced laboratories use a Cs fountain to calibrate the master clock. This rather complicated ensemble could be replaced by a single continuously operated clock exhibiting high stability and accuracy performances. Such a clock could also be used in the ground part of satellite navigation systems or for inertial navigation in submarines.

The Solution

In this project, industrially oriented solutions are proposed and realized to transfer these innovative techniques from laboratories to clock manufacturers. This will allow clocks manufacturers to implement and launch into the market new products exhibiting good performances and at the same time featuring paramount properties from an industrial point of view like portability, reliability and low power consumption. In addition, the clocks developed in this project, once properly engineered, may be used as on board clocks for the European satellite system GALILEO.

Impact

The project outputs have been shared widely with the metrology community and instrumentation and clock manufacturers. The innovative techniques and/or solutions have been presented to European clock manufacturers and space agencies. Demonstrating the technology and commercial potential of the new technologies will promote their use by clock makers and industry. The results will be useful to many institutes



or companies whose activity is related to accurate and stable time and frequency signals, including those wanting to have stable and high performing which are cheaper and more compact than at present.

2 Project context, rationale and objectives

Context

Optical clocks reached outstanding accuracies, at the level of 10^{-16} or even better (in terms of relative frequency), and it is expected that in 10 years the present definition of the SI second may change from the microwave domain (ground-state hyperfine frequency of Cs) to the optical one. However, these performances are well beyond what is required for most industrial applications. Moreover, optical clocks are in general not reliable devices and still at the level of laboratory prototypes in terms of size, cost and power consumption. Yet, more than accuracy, frequency stability is the main metrological parameter required by a clock in a number of scientific and practical applications. Considering that most of the industrial applications are still related to microwave frequencies, one can easily argue that microwave rather than optical clocks are interesting for present practical purposes. In the microwave domain, H-masers offer the best capabilities in terms of medium-long term stability but, again, they are bulky, very expensive and only a few laboratories can afford them. In practice, a clock with frequency stability of a H-maser (of 10^{-13} at 1 s and in the 10^{-15} range for measurement times up to one day) but with a much simpler physics system would be enough to assure the required performances in many nowadays and future applications.

Those applications include, for example, telecommunication, where the requirements for more stable frequency references are driven by demands for rapid data transfer via optical fibre.

In wireless communications as well, improved clock performance are required. In fact, the future wireless will include high-speed data and broadband transmission, high capacity to support a huge number of simultaneous users, global mobility, high security, and scalable quality of service along with low cost for both operators and subscribers. The above features are imposing technical challenges on system design and stimulating various research topics on capacity, complexity and performance.

Objectives

The project reviewed the performance and features of vapour-cell clocks (Rb clocks are a type of vapour-cell clock) including commercial and laboratory prototypes, and evaluated what industry requires now and in the future. The project then characterised and validated two specific types of vapour-cell clock, and examined a third option which is still in the research stage.

The project had the objectives:

- **To review the microwave vapour-cell clocks**, including both the commercial devices currently available on the market and the most recent clocks exploiting laser pumping techniques. The aim of the review is to identify the limitations of traditional commercial devices to fulfil the increasing demands of some advanced technological and industrial applications and to highlight the need to convert better performing laboratory vapour cell clocks into industrial products. In addition, the review will include input from the stakeholder committee which will address industrial needs and be fed into the project.
- **To develop a vapour-cell clock based on the pulsed optical pumping (POP) principle** with a fractional frequency stability of units of 10^{-13} at 1 s and in the 10^{-15} range at 10^5 s. The clock will be targeted on industrial applications in terms of size, power consumption and reliability.
- **To develop a vapour-cell clock based on cold atoms** with performances comparable to those of the pulsed optical pumping on the short term but with better performances on the long term including a metrological specification of accuracy within an order of magnitude of that of primary standards. The project will identify the compromises required in order to obtain the expected performance while still targeting industrial applications.
- **To investigate alternatives principles, such as coherent population trapping (CPT) or electromagnetically induced transparency**, to study the possibility to realize a clock optimized in terms of compactness and to provide support to the implementation of the previous clocks.

3 Research results

3.1 Review of the microwave vapour-cell clocks (commercial and research devices)

The aim of the review was to identify the limitations of traditional commercial devices to fulfil the increasing demands of some advanced technological and industrial applications and to highlight the need to convert better performing laboratory vapour cell clocks into industrial products.

Specifically, we considered the following commercial clocks which are produced by American and European manufacturers and currently used: PRS10 (Rubidium frequency standard made by Stanford Research Systems), SA.22c Precision Rubidium Oscillator (Symmetricom, USA), SA.22c-LN Low Noise Rubidium Oscillator (Symmetricom, USA, shown in Fig. 1(a)), (Symmetricom, USA), SA.3Xm Miniature Rubidium Atomic Clock (Symmetricom, USA), LNRclock – 1500 (Spectratime, Switzerland), Low Cost & Profile Frequency Rubidium Standard (LFRS, Spectratime, Switzerland, shown in Fig. 3.1(b)). These clocks are mainly used in telecommunications or synchronization applications. In general, they exhibit a frequency stability in the range of $(1\div 4)\times 10^{-11}(1s)$ and an aging $< 5\times 10^{-11}$ (monthly).



Fig. 3.1 Picture of SA.22c – LN (Symmetricom) (a) and of LFRS (Spectratime) (b).

However, with the increase of amount of data exchanged worldwide, the growing concerns on data integrity and security, with the increasing of applications requiring time stamping, it is expected that stable frequency references will be increasingly required. Definitely, the commercial vapour cell clocks are in general compact and low cost devices but they exhibit low frequency stability performances. More stable clocks are then needed for matching the requirement of modern applications, such as wireless high speed data transmission, satellite navigation, time synchronisation of networks for error-free data transfer. As a result, high frequency stability, low cost, low power consumption, low volume and mass are needed for industrial and commercial applications. The following Table 3.1 resumes typical performances of best laboratory-prototype vapour cell clocks. We clearly identify some prototypes with best frequency stability performances in the range of a few $10^{-13}\tau^{-1/2}$: the CW Rb clock (UNINE), the POP clock with optical detection (INRIM), the pulsed Cs CPT clock (OBSPARIS) and the cold-atom HORACE clock (OBSPARIS). These frequency standards present a high-potential for high-performance and compactness. Among them, current performances of the POP clock with optical detection (INRIM) and the pulsed Cs CPT clock (OBSPARIS) remain far from being at the shot noise level. The HORACE clock is of great interest for frequency accuracy. Consequently, it is thought that the three prototypes (POP clock, HORACE clock, Pulsed CPT) have a great potential for improvement and specific techniques or solutions have been studied in this project in order to make this clocks suitable to a commercial implementations.



Clock	FWHM (Hz)	SNR	C(%)	$\sigma_y(1s)$	$\sigma_y(10000\text{ s})$	FL(1s)
CW Rb Clock (UniNe)	361	2.2×10^5	25	2.4×10^{-13}	7×10^{-14}	5.5×10^{-14}
POP μw (INRIM)	54	200	100	1.2×10^{-12}	3×10^{-14}	1×10^{-12}
POP opt (INRIM)	150	20000	33	1.7×10^{-13}	6×10^{-15}	2×10^{-14}
POP opt (China)	125	840	90	2×10^{-12}	2.5×10^{-14}	$< 1 \times 10^{-13}$
CPT maser (INRIM)	210	21000	100	3×10^{-12}	4×10^{-12}	7×10^{-13}
CW CPT (Zhu)	218	26000	22	1.5×10^{-12}	2×10^{-13}	x
CW CPT (Knappe)	100	1100	x	1×10^{-11}	2×10^{-12}	x
Pulsed CPT (OBSPARIS)	125	40000	12	6×10^{-13}	3×10^{-14}	2×10^{-14}
HORACE (OBSPARIS)	20	900	x	2.2×10^{-13}	5×10^{-15}	1×10^{-13}

Table 3.1: Resume of best laboratory-prototype vapour cell clocks typical performances. FWHM: clock signal linewidth, SNR: signal to noise ratio of the clock resonance in a 1 Hz bandwidth, C: contrast of the resonance = ratio between the signal peak-peak height and the dc background, FL: fundamental limit (shot noise or thermal noise), best achievable frequency stability at 1 s, x: not known or not measured.

Among the different solutions which were investigated, the magnetron-type cavity developed in UniNe is very interesting and we consider it as an original alternative to help the POP clock to be smaller in volume. A simple-design architecture should be favoured for the pulsed Cs CPT clock to be compliant with industrial transfer. Interesting techniques proposed in that sense by UFC have been studied in detail in the project. A cold-atom clock based on HORACE principle has been developed with the Rb atom. This allows to develop the optical setup using frequency-doubled 1.5 μm telecom-domain fibre components to be fully compliant with industrial requirements.

All partners have participated in the review; specifically, they all contributed in the search for bibliographic documents, including clocks data sheets in the companies' websites, and in the analysis of the documents themselves.

3.2 Development of a Pulsed Optically Pumped Rb frequency standard

The aim was to develop a compact vapour-cell clock based on the pulsed optical pumping approach. The added value of the pulsed approach is that the atoms make the clock transition in the dark, when the laser light is off. In this way laser instabilities are not transferred to the atoms with great benefit for the clock's frequency stability. The expected fractional frequency instability for such a clock was at the level of few units of 10^{-13} at 1 s, reaching the 10^{-15} range in the medium-long term period. In order to match industrial requirements, innovative solutions will be adopted in the clock design, in terms of size, power consumption, insensitive to environment fluctuation and capability to operate in industrial field.

A proper industrialization of such a clock will cover then an important market sector with a low cost and high-reliable device. Specifically, the POP clock candidates as a master clock in a network of synchronized clocks (telecommunication, satellite radio-navigation such as GALILEO, etc.) where long-term stability is a main issue.

In the development of the POP clock, INRIM contributed by designing, implementing and testing the physics package, UniNe by realizing the quartz cell and the magnetron cavity, UFC in contributing to design and realize the low phase noise electronics. OBSPARIS, gave some useful suggestion to realize the optical setup.

Development of a prototype of POP Rb clock

The POP Rb clock is composed of three subunits: the physics package, the optical system and the electronics. The specifications for each unit have been given according to the results obtained at INRIM with a previous prototype of POP Rb clock.

The **physics package** (PP) is the core of the clock since it contains the alkali-atom vapour cell. We designed, develop and test the PP components and assembled them. This work has been jointly done by INRIM and



UniNe. The physics package will be optimized concerning its size, in fact a magnetron cavity allows a significant reduction in size in comparison to a more traditional microwave cavity. From the innermost to the outmost, the following components can be identified:

- 1) Clock cell;
- 2) Microwave magnetron cavity;
- 3) Thermal ovens
- 4) Magnetic shields

Two quartz cells (no. 3300 and 3301) have been produced for use in the Mclocks POP clock. Nominal specifications for the cells are an isotopic content of ^{87}Rb (Rubidium 87) and a mixed buffer-gas (Argon (Ar) and Nitrogen (N_2) with a pressure ratio PAr: $\text{PN}_2 = 1.6$) and overall pressure of 25 torr (or 33 mbar @ 60 °C). The cells have been tested using a CPT arrangement.



Fig. 3.2 Clock cells for the Mclock project filled and characterized by UniNe.

According to the buffer pressure shifts of ^{87}Rb in Argon and Nitrogen and the known cell filling parameters (pressure ratio: PAr: $\text{PN}_2=1.6$), the mixed buffer gas pressure shift at 40 °C is calculated as 173 Hz Torr-1. The resulting total buffer-gas pressure in the cells is listed in Table 3.2. The calculated total buffer-gas pressure corresponds well to the 25 torr total pressure aimed for in the cell production.

Cell no.	Intrinsic clock frequency	Total buffer-gas pressure (at 60°C)
3300	4234(1) Hz	26.06 torr
3301	4248(1) Hz	26.14 torr

Table 3.2. Measured clock frequency shift for the two cells

From the spectroscopic tests results, both cells produced for the POP clock (no. 3300 and 3301) showed enriched ^{87}Rb (more than 95%) content and met all the design requirements for the buffer gas content. The cells successfully passed these first spectroscopic tests that aimed at a first screening of the cell quality. The cells were then integrated into the magnetron cavity.

UniNe has also developed a highly compact magnetron cavity for operation in the POP clock. A photograph of this cavity type's main body is shown in Figure 3.3a. In this design, a set of 6 metallic electrodes placed inside the cavity and surrounding the Rb vapour cell are used to achieve the desired well-defined TE_{011} -like

mode structure of the microwave magnetic field, as well as correct frequency tuning to the ≈ 6.835 GHz frequency of the ^{87}Rb clock transition. Figure 1b shows a numerical simulation result for the microwave magnetic field distribution inside the cavity, at the 6.835 GHz resonance frequency. This cavity design is of high interest for the realization of the Mclocks POP because of its very low volume of 44 cm^3 only, which is a factor of 3 smaller than the hollow-cylinder cavity of 140 cm^3 volume applied in previous state-of-the-art POP clock.

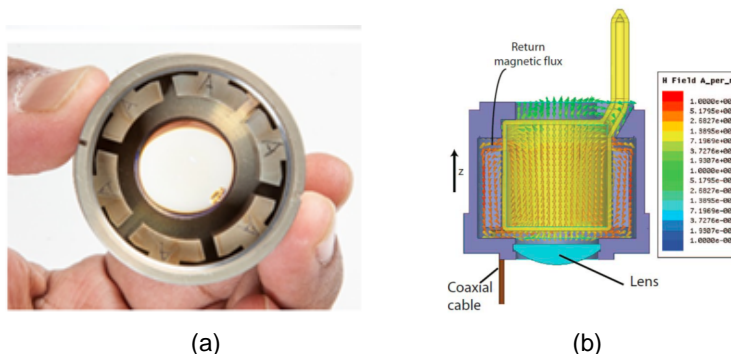


Fig. 3.3. Photograph (a) and field simulation results (b) for the compact magnetron cavity.

In order to gain experimental insight on the magnetron cavity operation with the cell design of Fig. 3.2, the microwave resonance frequency of the magnetron cavity has been measured. Figure 3.4 shows an example of the measured cavity resonance response, in terms of microwave power reflected by the cavity (vertical axis in Fig. 3.4) as function of incident microwave frequency (horizontal axis in Fig. 3.4). Full frequency span shown is 100 MHz, with 6.834 GHz center frequency. Measured quality factors are on the order of 230. These results thus confirm the expectations from the numerical simulations shown in Fig. 3.3b.

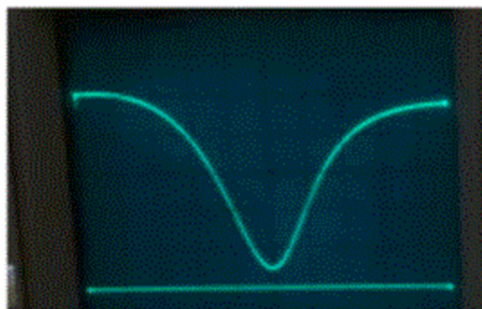


Fig. 3.4. Experimental measurement of the microwave cavity resonance. Vertical axis gives reflected microwave power, horizontal scale microwave frequency. Center frequency is 6.834 GHz, span is 100 MHz.

The microwave cavity resonator has been mounted in the clock PP (see Fig. 3.5) and the clock prototype has been characterized (see following subsection).



Fig. 3.5. Photographs of the microwave cavity during integration into the clock PP.

The **compact laser system** for the POP clock was manufactured and assembled by UniNe, according to the specifications given by INRIM.

Here is a list of the main functions and elements of the laser system:

- Laser emission on the Rb D2 line (780 nm) provided with a Distributed Feed-Back (DFB) laser diode.
- To prevent unwanted feed-back to the laser diode, an optical isolator has been implemented at the output of the laser.
- Frequency-stabilization of the laser emission to the Rb atomic reference lines integrated into the laser system using an evacuated reference Rb cell.
- The reference Rb cell can be heated to increase the atomic absorption signal and has a magnetic shielding.
- A pulsed (switched) optical output of the laser system, using an acousto-optical modulator integrated into the laser system.
- Reduction of the laser beam size with a telescope in order to increase the acousto-optical modulator efficiency.
- The acousto-optical modulator can be used in double-pass configuration, allowing a frequency shift up to 200 MHz.
- Integration of the pre-amplification circuits for the photo-detectors into the laser system.
- For a good thermal equilibrium and in order to reach the best long-term frequency stability, all components will be mounted on a heated thermally controlled baseplate.
- Pin-pin compatibility of the electronics interface connections of the laser system to the laser control electronics previously delivered to INRIM by UniNe.

The CAD design drawing of the laser system and the fully assembled laser system are shown in Fig. 3.6 below.

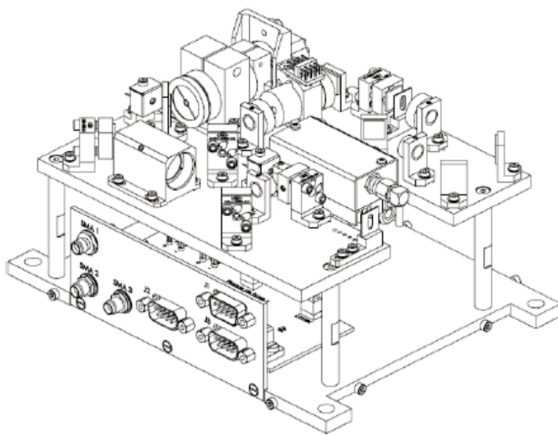


Fig. 3.6. Fully assembled laser system.

All components are mounted on a heated thermally controlled baseplate. The laser assembly consists in a DFB laser diode with integrated Peltier element and a collimating lens. The optical isolator avoids unwanted light feed-back into the laser chip. The reference Rb cell provides a strong and narrow saturated-absorption signal on which the laser is frequency stabilized. To increase this absorption signal, the cell is heated to a temperature of about 40°C. The cell is also surrounded by two magnetic shields in order to protect the atoms from any external magnetic disturbances. The telescope reduces the diameter of the laser beam from 3-4 mm to < 1 mm in order to increase the Acousto-Optic-Modulator (AOM) efficiency and to be able to separate the 0, ± 1 and ± 2 diffraction orders from each other. The AOM is set in a double-pass configuration that allows shifting the light's frequency twice the value of the RF fed to the AOM, without affection the direction (angle) of the laser beam at the output of the laser system. Two beam blockers are placed just before the retroreflective



mirror and at the optical output of the laser system, in order to select the appropriate diffraction orders for the experiment.

The laser system occupies a total volume of about 2.3 litres, of which 1.0 litres are occupied by the optical setup while the remaining volume (1.2 litres) at this phase is dedicated to accommodate proximity electronics and could be reduced in future development steps.

The photodetector and fixed mirror at the reference Rb cell can be removed and the additional optical outputs used in order to implement external optical elements for variations of the laser stabilization scheme. The laser system has been extensively tested. In particular, the laser system output power has been measured at 15 mW at 100 mA. The laser current can be safely increased up to 130 mA if more output power is needed (obviously, the laser temperature should be adjusted to reach Rb absorption). The ON/OFF ratio has been measured at 40 dB (ON = 12 mW, OFF = 1 μ W). However this measurement is quite sensitive to the background light in the laboratory, and the measured ON/OFF ratio might be limited by this effect.

This measurement has been performed by switching ON/OFF the RF power at a frequency of 10 kHz. The graph below shows an AOM rise/fall time of 4.5 μ s, that corresponds to the time interval measured between 10% and 90% of the maximum light signal. The rise/fall time specification of the RF switch used is typically 5 ns and the switching time is typically 10 ns. Therefore the measured rise/fall times are not limited by the switch. The linewidth of the laser system has been measured using the beat signal between the laser system's output beam and a reference laser head (Fig. 3.7). Both laser systems use DFB laser diodes of same type and supplier, and were free running during the measurement. The beat width has been measured at 3.4 MHz \pm 0.3 MHz, which corresponds to a linewidth of 1.7 MHz for each individual laser.

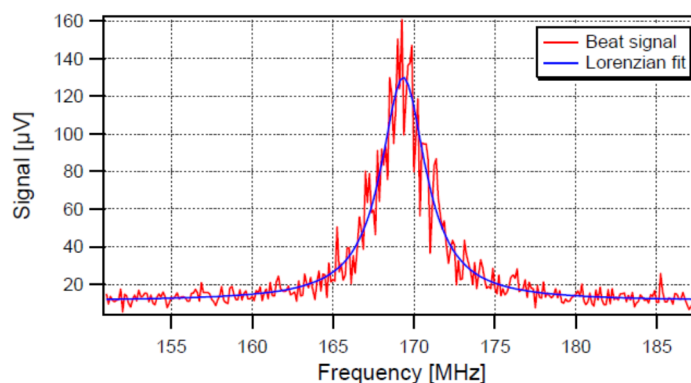


Fig. 3.7. Beat note between the laser system and a laser head. The two laser systems use DFBs of same type. The beat width is measured at 3.4 MHz \pm 0.3 MHz.

The frequency stability was also measured by beat note between the laser system and a reference laser head. Both lasers were locked on the same atomic transition (cross-over 21-23), the beat frequency then corresponds to the -160 MHz AOM shift of the laser system. Figure 3.8 shows the beat frequency stability measurement of about 90 hours. At 1 second, the relative stability is 1.5×10^{-11} and stays below 1×10^{-11} from 3 seconds to 10^5 seconds. A bump is present from 1'000 to 10'000 seconds, which is due to thermal variations in the laboratory.

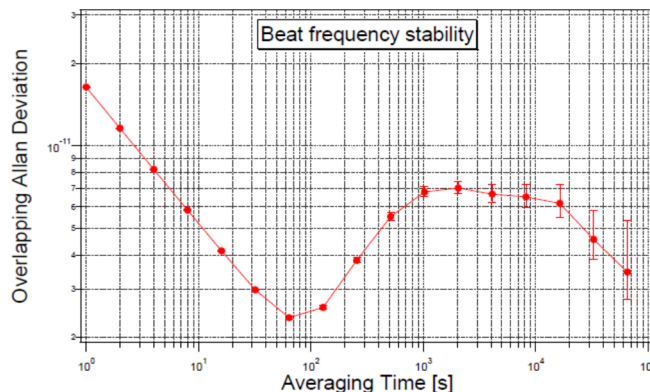


Fig. 3.8. Frequency stability of the beat note between the laser system and the reference laser head.

The relative intensity noise of the system has been measured before and after double pass through the AOM. Before double pass (see blue curve on Fig. 3.9), the Relative Intensity Noise (RIN) behaviour is the same as the laser diode alone. However, after the double pass through the AOM, the noise level is increased in the frequency band between 10 Hz and 5 kHz. The slight increase of noise after 20 kHz is due to the noise limit of the external detector used for the measurement.

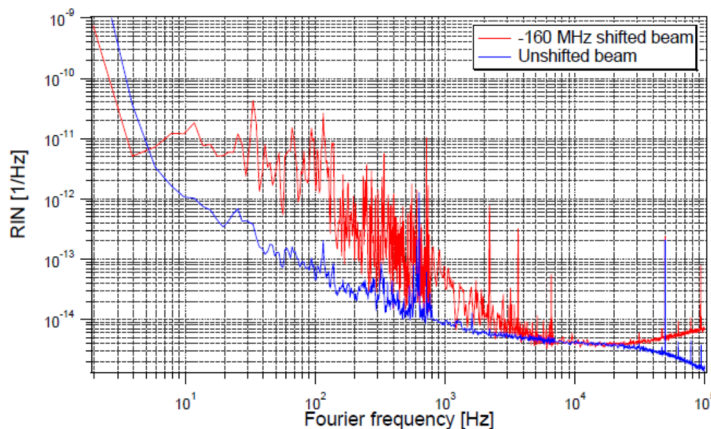


Fig. 3.9. RIN of the laser system, measured before (blue) and after (red) AOM.

To run the clock a suitable electronics has been implemented; this electronics includes a synthesis chain and a control electronics to control the main clock's parameters like temperature, magnetic field, etc. Most of this work has been done in collaboration with UFC. Figure 3.10 shows the synthesis chain architecture.

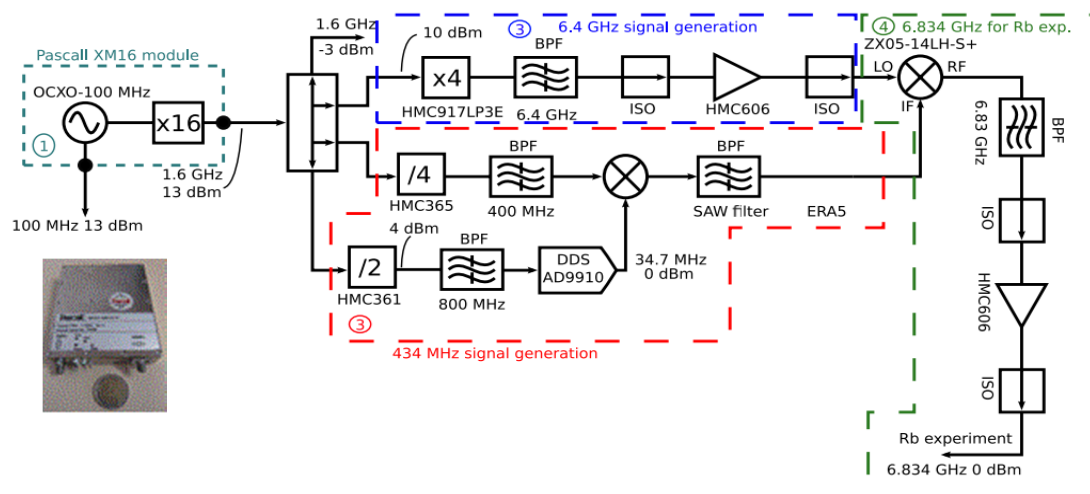


Fig. 3.10. Architecture of the POP clock synthesis chain.

The pilot and key element of the synthesis chain is a low phase noise XM16 Pascall module. It integrates an ultra-low phase noise 100 MHz Oven Controlled Cristal Oscillator OCXO (similar to the one used in the CPT clock synthesis chain) and a multiplication stage to produce a low noise 1.6 GHz output signal with a power of 13 dBm. This signal is divided into 4 arms with a power splitter. In the first arm, the 1.6 GHz signal is multiplied to 6.4 GHz with a low noise frequency multiplier (Hittite HMC917LP3E). The output signal is bandpass filtered with a 50 MHz-bandwidth bandpass filter and isolated with a microwave isolator to prevent feedback. In the second arm, the 1.6 GHz signal is frequency-divided by 4 with a low noise frequency divider (Hittite HMC365G8) to produce a 400MHz signal. In the third arm, the 1.6 GHz signal is frequency-divided by 2 with a Hittite HMC361S8G to an output frequency of 800 MHz. The fourth output is kept to deliver an output signal of 1.6 GHz.

The 800 MHz output signal is used to drive a direct digital synthesis (AD9910) that generates an output frequency of 34 MHz. This signal is mixed with the output 400 MHz signal in a single-sideband mixer in order to generate a 434 MHz signal. This 434 MHz signal is mixed with the 6.4 GHz signal in a microwave mixer (MMP12241) to generate the final 6.834 GHz signal used to probe the atomic resonator. This 6.834 GHz signal is band pass filtered, isolated and amplifier with a low noise microwave amplifier (ZX60-183-S+).

The 100 MHz OCXO pilot frequency can be tuned with a voltage in the 0-10 V range to be locked to the atomic transition frequency.

Clock characterization

Once assembled, the POP Rb clock (INRIM version with traditional cylindrical cavity) looks like in Fig. 3.11.

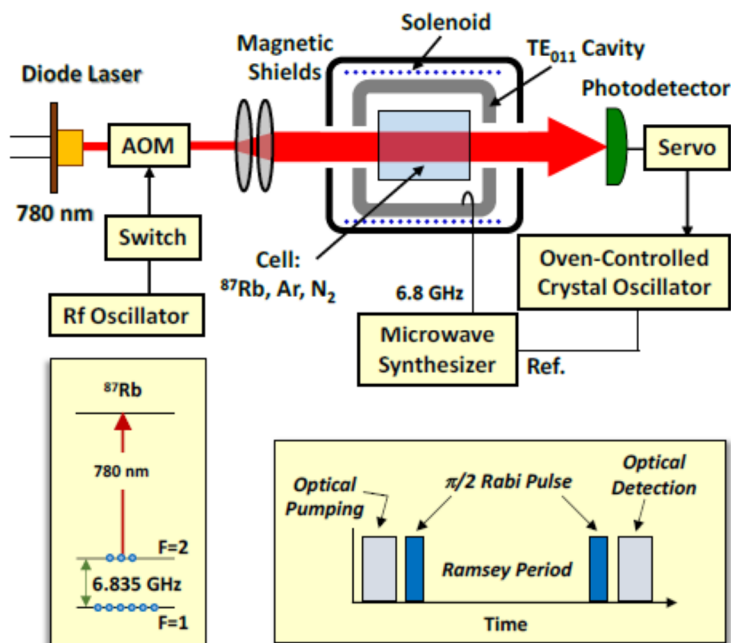


Fig. 3.11. Illustration of the components for INRIM's pulsed-laser Rb clock.

In our pulsed optical pumping experiments, the durations of the three interrogation phases are set as follows: 1. Pumping time $T_p=0.4$ ms; 2. Microwave pulse time $T_1=0.4$ ms; 3. Ramsey time $T_{\text{Ramsey}}= 3$ ms; 4. Optical detection time $T_d=0.3$ ms. The total cycle period T_c is 4.54 ms (including some pauses). The vapour cell temperature is fixed at 64 °C.

A preliminary evaluation of the clock prototype was performed by using the response from the Rb atoms in the cell, notably by measuring Rabi oscillations and the clock signal in Ramsey interrogation mode.

Figure 3.12 shows the Rabi oscillations observed for the clock prototype, in terms of contrast of the central Ramsey signal fringe as a function of microwave pulse area. The observation of the clear Rabi oscillations and their slow wash-out with increasing microwave pulse area indicates a highly homogeneous microwave magnetic field amplitude across the cell inside the cavity, as required for the POP clock.

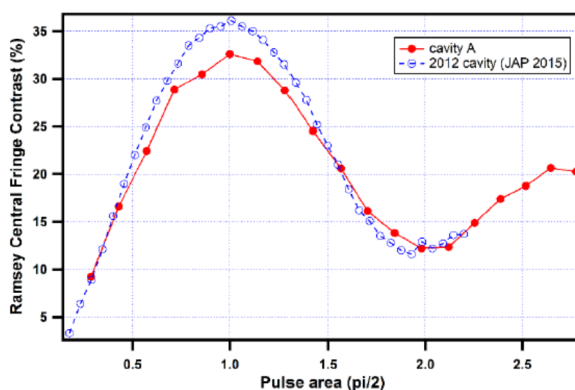


Fig. 3.12. Rabi oscillations measured for the clock prototype at UniNE (Red bullet). A comparison is done with a previously realized magnetron cavity (blue open bullet).

Figure 3.13 shows an example of the Ramsey fringes detected in our clock by the optical detector.

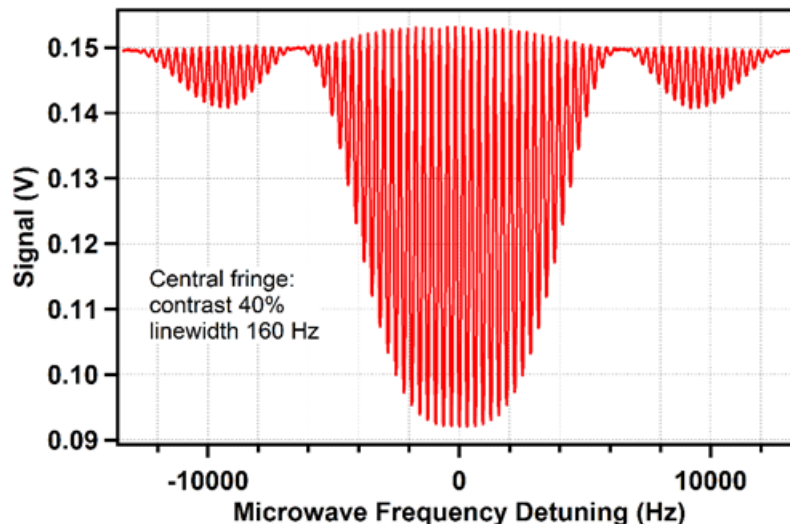


Fig. 3.13. Ramsey pattern observed on the Rb clock transition, for the assembled clock prototype.

The laser's pumping power is around 15 mW and the detection power is 1.2 mW. The central fringe contrast is of 35% and its full-width at half maximum (FWHM) $\Delta\nu$ is 160 Hz which is consistent with the theoretical prediction $\Delta\nu=1/ T_{Ramsey}$. Using these results from the Ramsey fringes, the shot-noise limited short-term stability with optical detection can be inferred. The shot noise limit can be expressed as:

$$\sigma_y^{sn}(\tau) = \frac{1}{\pi Q_a R_{sn}} \sqrt{\frac{T_c}{\tau}}$$

where Q_a is the quality factor of the clock transition ($\approx 4.3 \times 10^7$) and T_c is the cycle time. R_{sn} is the signal to noise ratio (SNR) defined as $R_{sn} = C \eta N_{opt}$ where C is the central Ramsey fringe contrast and η is the efficiency of the photo detector. N_{opt} is the number of optical photons during the detection time T_d . In our case, R_{sn} is at a level of 30000 and the final expected shot-noise stability limit is $1.7 \times 10^{-14} \tau^{-1/2}$.

Using the preliminary Ramsey contrast of 34 % recorded in early evaluations (see Fig. 3.13), the servo loop of the clock prototype was closed and a first short-term stability of the clock was measured. The result in Figure 3.14 shows a clean short-term clock stability of $3.0 \times 10^{-13} \tau^{-1/2}$.

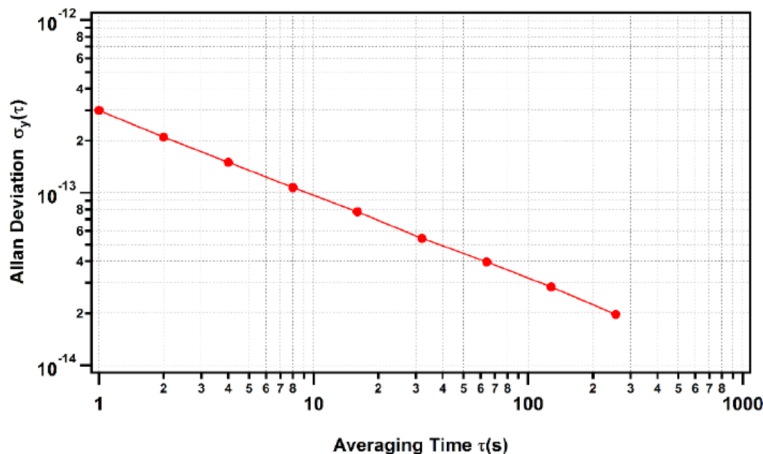


Fig. 3.14. Clock stability recorded for the POP clock prototype using the magnetron cavity.



In order to reduce the number of discrete components, we studied the possibility to lock the laser frequency using the same cell adopted for clock purposes. This has been done on another PP implemented at INRIM and optimized for medium-long term performances. In Fig. 3.3.1515a Ramsey fringes are also shown. The result is that the frequency stability is not significantly degraded and the level 8×10^{-15} is reached for integration times up to 4000 s.

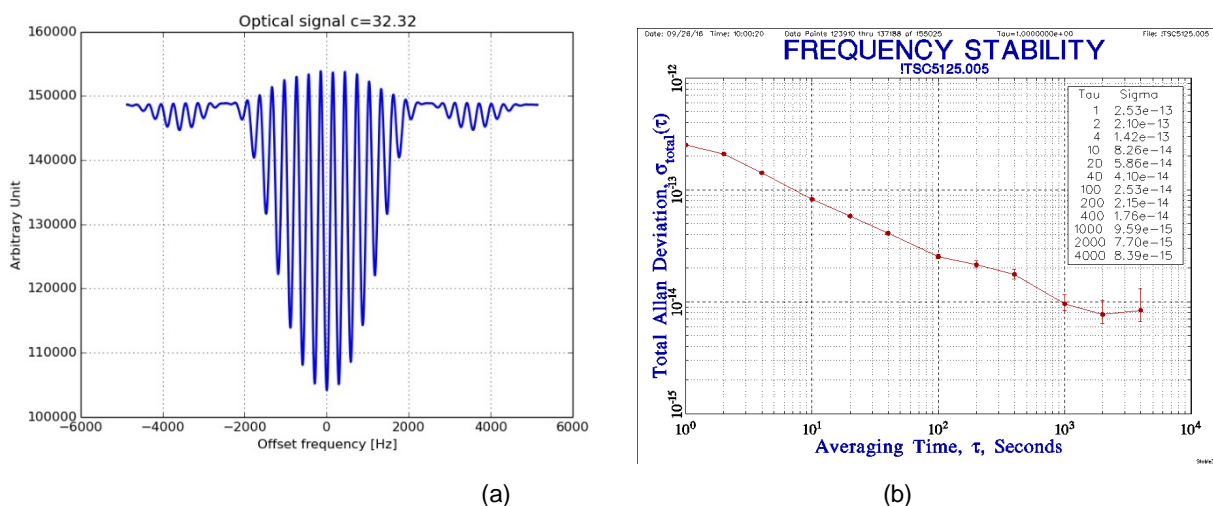


Fig. 3.15. Ramsey fringes and POP clock frequency stability when the laser frequency is locked on the cell clock.

3.3 Development of an industry-ready frequency standard based on cold Rb atoms

Another goal of the Mclocks project has been to develop a prototype of an atomic clock which could deliver a frequency stability at the level of units 10^{-13} (a 1s) while at the same time bringing an accuracy specification at the level of a few 10^{-15} which is inherently superior to the GPS+H-MASER systems currently in use. Furthermore, a key feature of this work has been to realize this development in a form which is from bottom-up geared towards an industrial development in terms of costs, size and projected reliability. More precisely, the prototype developed aimed at closing the existing gap between currently available commercial products and atomic fountains both in terms of stability and accuracy. This objective requires sacrificing in part the simplicity and miniaturization potential of the POP clock to allow the use of an ultracold atomic sample. This approach which might sound daunting and complex has been considerably simplified by the R&D carried out since almost two decades at OBSPARIS.

The operation of the clock is based on the Ramsey interrogation of a sample of ultracold (microkelvin temperature) Rubidium atoms in free fall inside a microwave cavity. Taking advantage of the so-called isotropic laser cooling, the atoms are cooled from a vapour directly inside the microwave cavity thereby eliminating the need of a separate cooling chamber. The use of ultracold atoms suppress most of the uncertainties related to atomic collisions and allows one to benefit from interrogation times of several tens of milliseconds. The laser system required to operate the clock uses roughly 0.1W of power split into seven single-mode optical fibres, six used only for cooling and one which is also used for detection. A prototype for this kind of clock has already been realized at OBSPARIS using Cesium (Cs), demonstrating a short-term stability in the range of 10^{-13} and long term stability in the range of 10^{-15} still limited by atomic collisions. The advantage of using Rb is that this limit should be easily overcome and accuracy should be limited only by effects related to the microwave cavity well in the low 10^{-15} range. A new clock is under active development at LNE-OBSPARIS on a conservative approach which recycles most of the development of the Cs clock using present-day industry-standard components.

The main point of innovation in this project has been the use of a laser system based on frequency doubling of a laser emitting in the telecom band. This fibre-based approach, which almost entirely eliminates the need



of discrete optical components, has demonstrated both performance and reliability even in the rather harsh environment of microgravity flights.

The main issues faced in this project concerned the physics package: the number of atoms probed by the clock strongly depends on the environmental temperature and the microwave cavity needs to be tuned during fabrication with a costly and lengthy process, furthermore an effort has been made to eliminate the need of discrete optics. Finally, a better microwave synthesis chain has been realized leading to an improvement of this specification.

OBSPARIS designed and implemented Rubiclock, Muquans developed COLMAR, the laser system used in Rubiclock. UFC and INRIM contributed to design and test the synthesis chain of Rubiclock, INRIM contributed in the accuracy evaluation, UniNe developed a system to easily tune the microwave cavity.

Clock implementation

As for the POP clock, Rubiclock is composed of three subsystems: physics package, laser system and microwave synthesis. Resonator and synthesis have been made at OBSPARIS, and the laser system has been developed by Muquans (unfunded industrial partner).

The **physics package** is composed of several sub-systems. Main of them are the atomic resonator with its 3 magnetic shields. Inside the atomic resonator, we find the microwave cavity and the vacuum chamber, where the atoms are cooled, interrogated and detected. Vacuum chamber is mainly in titanium, allowing use of commercial components as dispenser and pumps, and the upper part is surrounded by the microwave cavity. To perform the isotropic light cooling, the upper part of the chamber is a fused silica bulb allowing optical access in all directions. The inner walls of the copper cavity act as an integrating sphere and 6 free-diverging fibres feed the cooling zone with cooling and re-pumping beams. To avoid loss of optical power along the vertical direction we add a vertical retro-reflected beam, which is also used as a detection beam.

Microwave cavity is tunable thanks to a copper ring at its top, allowing a tuning range of the resonance frequency of about 20 MHz.



Fig. 3.16. CAD of Rubiclock atomic resonator with its 3 magnetic shields. At the center, the fused silica bulb and the microwave cavity.

One of the key point of Rubiclock implementation, especially if we think to industrially convenient development, has been the realization of a system to fine tune the microwave cavity.

The precise resonance frequency of the microwave cavity used in the clock inevitably depends on the dielectric loading of the cavity with the dielectric material of the cell body.

Therefore, unavoidable small deviations in the cell geometry between different cells make it desirable to include into the cavity design a tuning mechanism that allows compensating for shifts of the resonance frequency introduced by such deviations in the cell realization. The novelty of the microwave cavity designed by OBSPARIS (SYRTE) for this project was to include such a tuning mechanism in to the cavity. The CAD design of the new spherical microwave cavities has been established by OBSPARIS and is shown in Fig. 3.17. The circular tuning ring that protrudes into the cavity volume acts as the tuning fixture for the cavity's resonance frequency. By inserting the tuning ring more or less into the cavity volume, the resonance frequency can be altered slightly. Thus mismatches in the resonance frequency from the precise Rb clock transition frequency due to unavoidable residual variations of the cell size can be compensated.

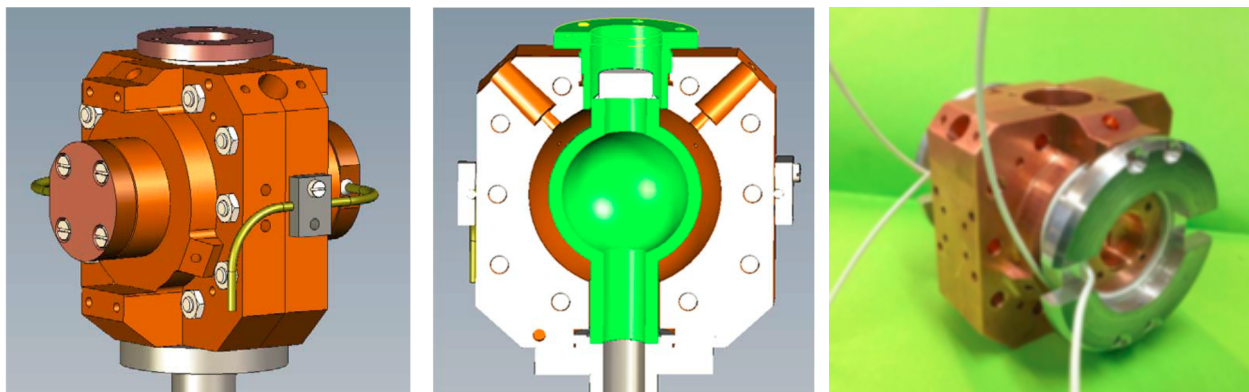


Fig. 3.17. Left: CAD design of the spherical microwave cavity. The tuning ring is seen on the top. Center: cut view of the cavity CAD design. The spherical cell body and the tuning ring are highlighted in green colour. Right: photograph of the assembled cavity (without tuning ring in place).

The cavity tests are undertaken using the transmission configuration, because the reflection configuration originally foreseen showed a very low signal-to-noise ratio, due to low coupling efficiency of the cavity resonances. All tests reported in this document were therefore conducted using the transmission configuration. The two identical microwave cables are chosen as input port (Port I) and output port (Port II). The microwave source is referenced to a local H-maser, and outputs a frequency scanning signal with the power of 0 dBm. The scanning span can cover the frequency up to 40 GHz. The transmitted signal is detected Port II using a power detector. The DC signal from the power detector and the ramp signal from the microwave source are then recorded simultaneously. In order to create a stable environment, the microwave cavity is placed in a temperature controlled oven whose temperature can be set between -90°C and 190°C. The temperature monitor is used to record the real temperature of the cavity.

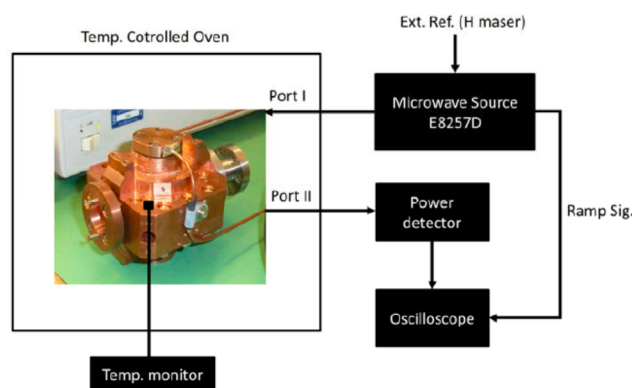


Fig. 3.18. Schematic of the cavity frequency test setup.

Simulations and experimental results (collaboration with UniNe) show that the resonance frequency can be adjusted with a copper ring.

The **laser system** has been developed by Muquans Company in collaboration with the Laboratoire Photonique, Numérique et Nanosciences LP2N. This system uses some reliable fibered telecom components at 1.5 μm , followed by a frequency doubling stage to reach the 780 nm rubidium D2 line. It generates more than 200 mW of optical power at 780nm, providing all the beams and frequencies needed for atom cooling, preparation and detection phases. New optical switches based on stepper technology, have been integrated in the laser system.

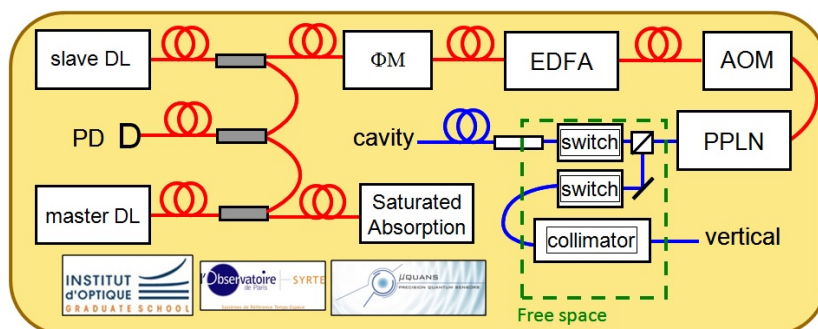


Fig. 3.19. Scheme of COLMAR.

Thanks to the use of fibered components, the whole setup including command electronics is very robust and compact (rack 19" x 6U, see Fig. 3.20). It has been tested and validated during 2 parabolic flights campaigns.

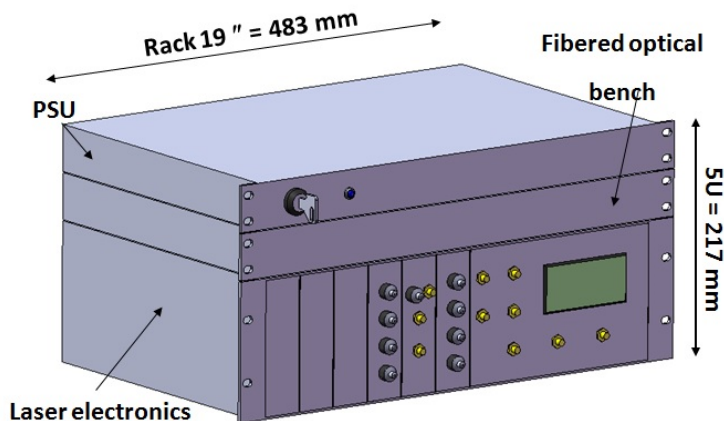


Fig. 3.20. Rack which houses the COLMAR laser system.

The microwave **synthesis chain** has been designed by SYRTE's Electronic Service. The local oscillator is a 10 MHz AR quartz. Specifications are compliant with a Dick effect less than 2×10^{-13} . The Synthesis uses a Phase Lock Loop PLL)-Dielectric Resonator Oscillator DRO (to generate a 7 GHz signal. A DDS signal is mixed to reach the 6.8 GHz clock frequency. A second DDS is used to control the frequency of a second output needed to generate the repumping beam of the laser system. This synthesis has been characterized and it does not degrade the noise of local oscillator. This setup has been integrated in a 3U rack.

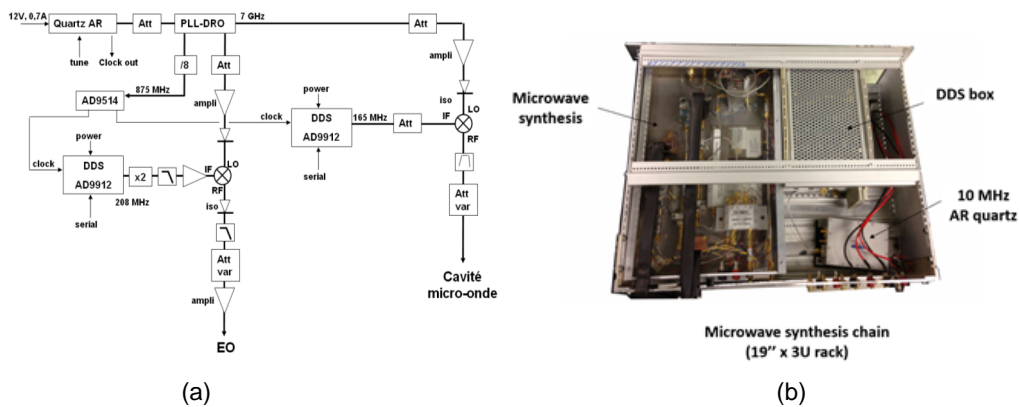


Fig. 3.21. (a) Scheme of the synthesis chain developed for Rubiclock; (b) the device in its box.

Clock characterization

Rubiclock participated in 6 parabolic flights (Fig. 3.22), validating all the sub-systems and the technological choices.

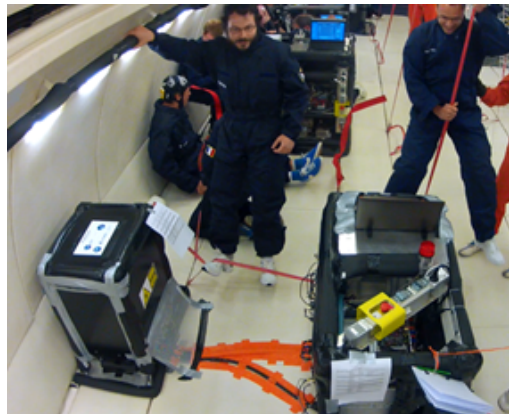


Fig 3.22. Luigi De Sarlo and David Holleville floating with Rubiclock during a 0g flight.

Thanks to microgravity, the clock can operate with longer interrogation times than in the lab, with a great win of the fringe contrast (see Fig. 3.23). In the same way, fringes with Ramsey interrogation time up to 400 ms has been demonstrated, but signal-to-noise ratio (SNR) was limited by the fluctuations of acceleration in the 0g plane.

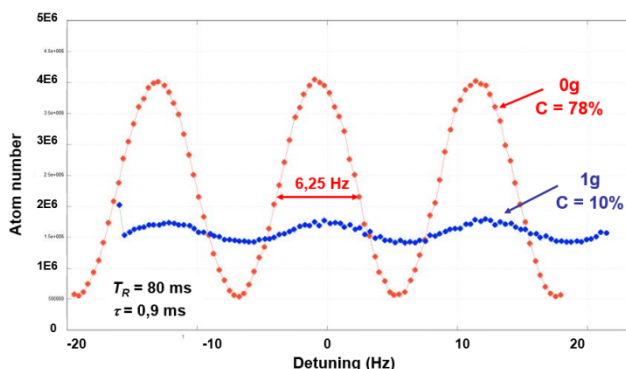


Fig. 3.23. Ramsey fringe with a 80 ms interrogation time on Earth and in microgravity. Fringe contrast is greatly improved in microgravity.

A lot of work in the lab to reduce the noise sources and to increase the SNR. The quantum projection noise has been reached and shot-to-shot Ramsey fringe SNR up to 1500 has been observed (see Fig. 3.24).

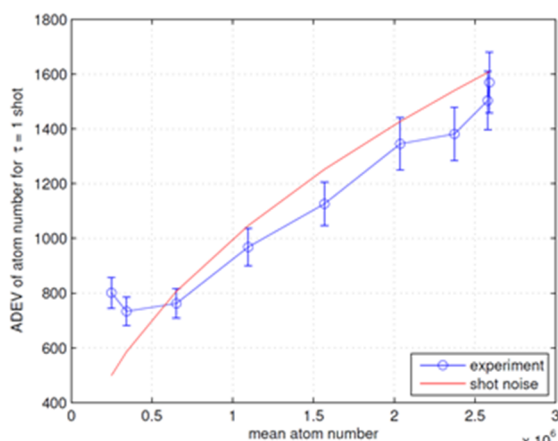


Fig. 3.24. Measured shot-to-shot detected atom number fluctuations (blue) vs. atom number (red) estimated ultimate quantum noise.

These very good results lead to a short term stability in the low 10^{-13} range (Fig. 3.25).

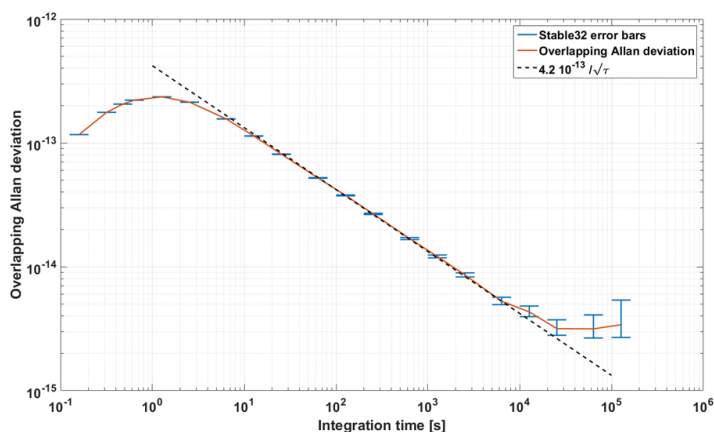


Fig. 3.25. Frequency stability of Rubiclock

The reasons of the drift are under investigations; a preliminary analysis shows that it could be related to a drift of the quantization magnetic field.

3.4 CPT alternative approach

Coherent population trapping (CPT) is a new attractive and simple way of interrogating the atoms and detecting the clock transition. In a CPT Cs clock, a vapour cell is crossed by two superimposed laser beams 9 GHz apart in frequency. Then there is no microwave cavity, the microwave frequency is, in a sense, optically carried by the laser beams. The clock signal is given by the record of the optical power transmitted through the cell. The atoms are pumped, interrogated, and detected by the same laser beams simultaneously. The design therefore is of great simplicity, well adapted to an industrial clock, making this technology very promising for compact atomic clocks.

In this project we have developed a CPT atomic clock compliant with industrial environment, after having analysed and separately tested several industry components.

The overall idea has been to develop a compact Cs vapour cell clock combining an optimized CPT pumping scheme (push-pull optical pumping) eventually improved by a pulsed Ramsey interaction. High-contrast CPT resonances will be detected using a dual-frequency dual-polarization modulated laser source. The detection of narrow resonances will be allowed by Ramsey interaction. The fractional frequency instability is expected to be around $5 \cdot 10^{-13}$ level at 1 s down to 10^{-14} range. Innovative solutions have been adopted in the clock to combine a small volume and reduced power consumption in a simple, compact and stable design using as many industry components as possible.

UFC and OBSPARIS designed, realized and implemented the physics package and the optical set-up. INRIM and UFC developed the synthesis chain and the control electronics, Tubitak contributed in the definition of the specifications of the CPT clock and in the study of CPT resonances in an open Lambda system. UniNe mainly contributed by characterizing the CPT cells.

Clock implementation

The atomic resonator includes the cell, a thermal regulation of the cell, a solenoid to generate the static magnetic field, and magnetic shields. The Cs vapour cell is the heart of the clock. Its characteristics directly impact on the clock performances.

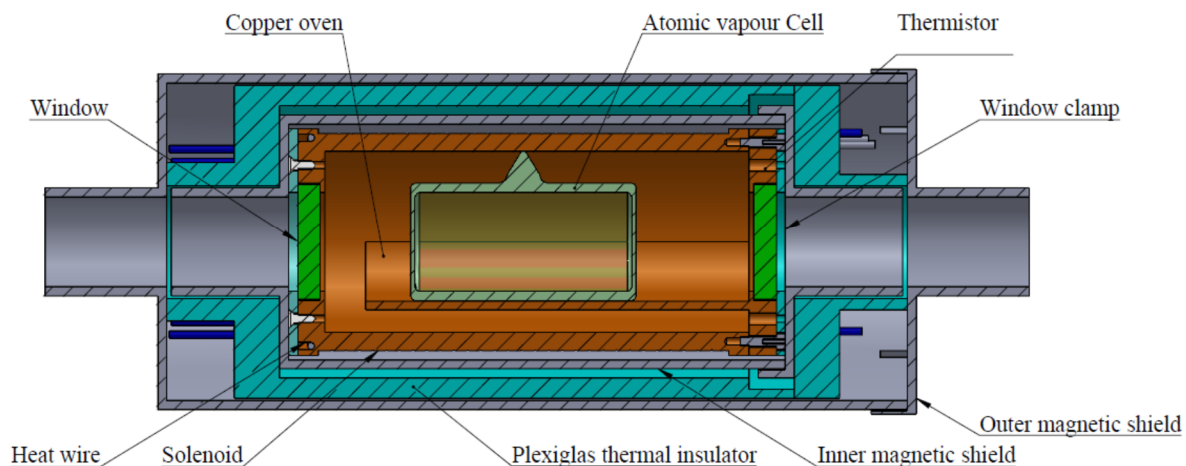


Fig. 3.26. Physics package scheme

The overview of cell physics package is shown in Fig. 3.26. There are several main considerations in this design: 1) the size of whole package should be as compact as possible; 2) the uniformity of the quantization magnetic field in the cell region should be high enough, so that the broadening of CPT spectrum of clock transition caused by it can be neglected; 3) the thermal regulation of the cell should be nonmagnetic, uniform and low power consumption; 4) the magnetic shields provide high shield factor of earth and other stray

magnetic field; 5) the demagnetization wire get through the cell package offer the function of demagnetization the magnetic shields whenever it is needed.

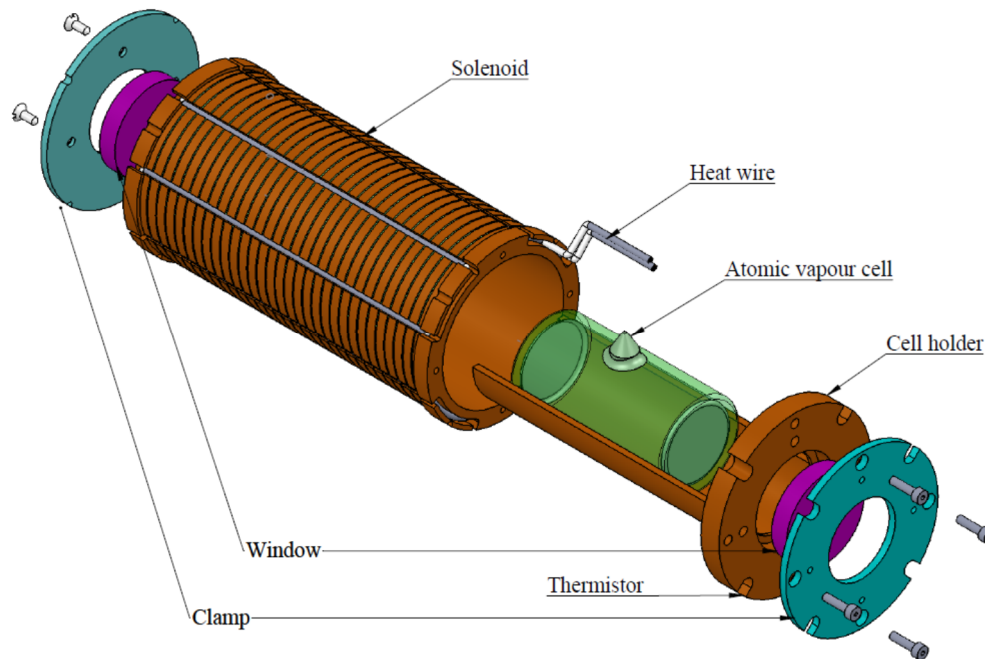


Fig. 3.27. Physics package scheme: inner part.

Figure 3.27 shows inner part of physics package. The copper oven is formed by two parts: heat cylinder and cell holder, which is adapted for the irregular stem shape and size of atomic vapour cell. The cell is mounted on the cell holder with its stem up, which is untouched with the holder for avoiding the atom Cs condense on the cell head and end faces. The heat wire with coaxial cable is nonmagnetic and can be placed into the inner magnet shield, thus the heat efficient is high. In reality, the coaxial heat wire is non-ideal, there is part of magnetic field leak from the cable when it is injected current. We found a geometrical winding configuration as shown in our design of Fig. 3.27 provides the minimum leak. For higher heat efficient, the two parts of copper oven contact with large area and screwed together.

In the CPT clock setup, the generation of optical sidebands is realized thanks to a pigtailed Mach-Zehnder electro-optic modulator. Mach-Zehnder electro-optic modulators are high-performance components used in a broad range of applications including high-rate optical telecommunications, chaos cryptography, optoelectronic oscillators and non-linear optics. Such devices allow to control the power of a laser beam by electrical control via the electro-optic effect of the differential optical path in a Mach-Zehnder interferometer, usually in a LiNbO₃ optical waveguide. They are of significant interest compared to bulk amplitude Electro-Optic Modulator EOMs for their compacity, ease-of-use, modulation bandwidth capabilities up to a few tens of GHz, low voltages and low insertion losses.

The reference of the MZ EOM used in our experiment is Photline NIR-MX-800 LN 10. This is a high bandwidth intensity modulator especially designed for operation in the 800 nm wavelength band. This Mach-Zehnder modulator working at 894 nm offers intrinsic and unparalleled benefits of LiNbO₃ (Lithium niobate) external modulation: high bandwidth, high contrast and ease of use. The NIR-MX800 exhibits a stable behaviour and supports several tens mW of input optical power. The MZ EOM uses polarization maintaining (PM) fibres with FC/APC fibres connectors (key parallel to the slow axis). Insertion losses are about 3 dB. The dc voltage is 3.2 V. The extinction ratio was measured to be 24 dB. Recently, thanks to a specific selection of Photline company on their EOM chips, we acquired a MZ EOM with extinction ratio measured to be higher than 39 dB by the manufacturer. Results presented here were obtained with the EOM with 24 dB extinction ratio.

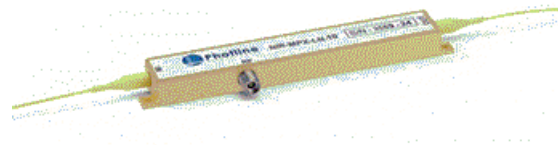


Fig. 3.28. MZ EOM used in the CPT experiment.

Laser intensity noise and fluctuations are expected to be a strong limitation to the clock short-term and mid-term frequency stability. In this experiment, we observed that the laser relative intensity noise at the direct output of the EOM is directly dependent on the EOM dc bias voltage, i. e on the transmission transfer function operation point. Figure 11 shows the laser RIN at the output of the EOM for six different values of the EOM dc bias voltage. The number on the graph is an indication on the optical power contained in first-order optical sidebands relative to the total laser power. For simplification, we neglect the optical power contained in high-order harmonics sidebands and we assume that the optical spectrum at the output of the EOM only contains the optical carrier and both first-order sidebands. The case where the power in sidebands is maximized and the power in the carrier is about null is normalized to 1 (case (1)). At the opposite, for the case (0), the optical carrier power is maximized and the power of sidebands is about null. The laser RIN at the input of the EOM is reported on the same figure for reference and comparison. We measured that the RIN at the output of the EOM is minimized and equals the input laser RIN when the total optical power contained in both first-order sidebands equals the optical carrier power (case 0.46). The RIN at the output of the EOM is degraded by about 5 dB when the power contained in each optical line is about equal (case 0.61). Most significantly, a significant degradation of about 15 dB of the laser RIN is measured at the output of the EOM when the optical carrier is optimally rejected (operation mode used in the present clock setup) or when the optical carrier is maximized and sidebands power nulled. Intermediate values of the RIN were measured for other intermediate values of the EOM bias voltage. The origin of this behaviour is not clearly understood at the moment and will require additional investigation. These results were found to be reproducible and were also observed in another MZ EOM-based CPT clock setup.

The electronics for the CPT clock is based on the same scheme used for the POP clock and will not be described here.

Clock characterization

The setup of the CPT clock is shown in Fig. 3.29.

The laser light is injected into a 10-20 GHz bandwidth polarization maintaining (PM) pigtailed Mach-Zehnder electro-optic modulator (MZ-EOM). The latter is a key component of the system. This single device allows both the generation of optical sidebands for CPT interaction and the on-off light switch for Ramsey interaction. The EOM is driven at 4.596 GHz by a low noise microwave oscillator to generate CPT sidebands frequency-separated by 9.192 GHz. A dc-voltage applied to the EOM bias electrode is adjusted so that the optical carrier is suppressed with a high-extinction ratio, in order to get an optical spectrum with two optical lines only. The EOM bias voltage can be actively controlled to stabilise the EOM transfer function operating point. At the output of the EOM, the modulated light has a linear polarization which is converted into alternating circular polarizations thanks to a Michelson interferometer. The incident beam is divided into two sub-beams in two different arms each containing a quarter-wave plate and a mirror. A fine adjustment of both quarter-wave plates followed by another half-wave plate allows to get time-delayed orthogonal states of linear polarisation at the output of the cube. An optical path difference $\Delta L = \lambda_0/4$ of about 8.1 mm (λ_0 being the clock transition wavelength) is adjusted between both arms in order to shift the intensity peaks of one beam by half a hyperfine period with respect to the peaks of the other. A quarter-wave plate is then inserted to get the output beam circular polarisation alternating between right and left.

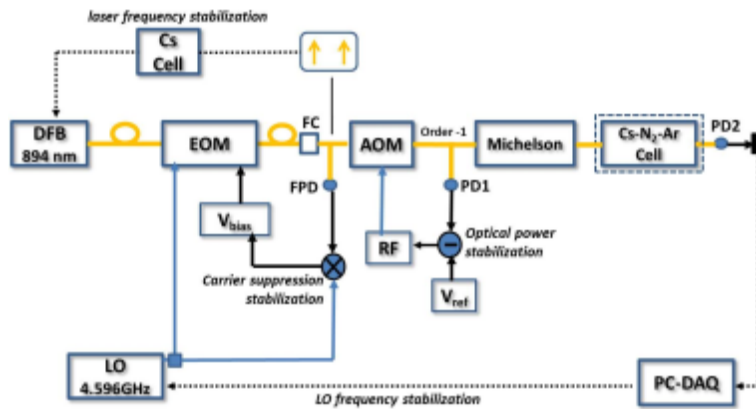


Fig. 3.29. Cs CPT clock experimental set-up

The short-term relative frequency stability $\sigma_y(\tau)$ of a passive atomic clock is well-approximated by:

$$\sigma_y(\tau) \sim \frac{\Delta\nu}{\nu_c} \frac{1}{SNR} \tau^{-1/2}$$

where $\Delta\nu$ is the clock resonance full-width at half maximum (FWHM), ν_c is the clock transition frequency, SNR is the signal-to-noise ratio in a 1 Hz bandwidth of the detected signal and τ is the integration time of the measurement.

Figure 3.30 reports the typical clock signal for an incident laser power P_L on the cell of 700 μW .

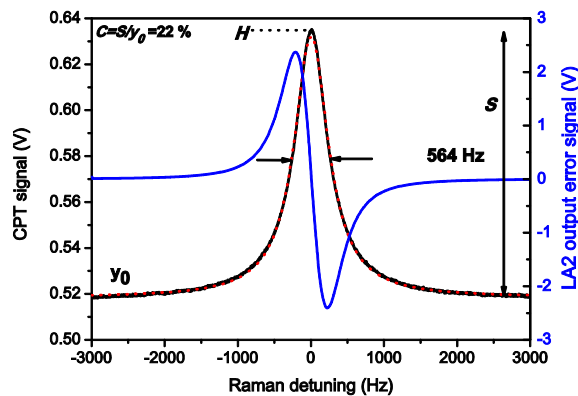


Fig. 3.30 CPT Clock signal (black) and its derivative (blue). The red dots are a fit by a Lorentzian function.

The clock resonance is well-fitted by a Lorentzian function. The CPT linewidth $\Delta\nu$ is 564 Hz. The clock signal S , defined on Fig. 3.30 as $S = H - y_0$, is 0.114 V. The resonance contrast C , defined as the ratio between the CPT signal S and the dc background y_0 , is 22%. The discriminator slope $D = S/\Delta\nu$ is measured to be 0.2 mV/Hz.

Figure 3.31 plots the Allan deviation of the clock frequency. The latter is measured to be 3×10^{-13} at 1 s, going down to about 3.2×10^{-14} at 100 s.

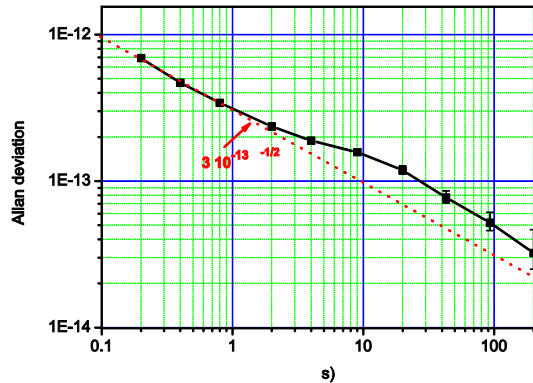


Fig. 3.31. Allan standard deviation of the CPT clock. Black squares: experimental data, red dashed line: expected stability for a white frequency noise fitted on the first points.

A large bump, from a few seconds to hundreds seconds averaging time, presently prevents the Allan deviation to decrease with a perfect white frequency noise slope. This is currently under investigation but could be explained by thermal effects (the laboratory room is not temperature stabilized), a non-optimized gain of the EOM bias voltage servo loop and feedback from the EOM fibre input face that slightly affects the laser frequency. An additional optical isolation stage should be added in a near future. Nevertheless, these short-term frequency stability performances, comparable to those of best vapour cell atomic clocks, are very encouraging for the development of a high-performance Cs vapour cell CPT atomic clock.

Table 3.3 shows main contributions to the clock short term frequency stability at $\tau = 1$ s. The noise budget is in excellent agreement with the measured clock fractional frequency stability. The clock frequency stability is currently mainly limited by the laser AM noise and the laser FM-AM noise process. The following contribution is the Dick effect. The latter will be reduced later thanks to a novel ultra-low noise frequency synthesis chain that should reject the Dick effect contribution to a level lower than 7×10^{-14} at 1 s.

TABLE 3.3. Main contributions to the clock short term frequency stability at $\tau=1$ s.

Noise source	$\sigma_y(1s)$
Shot noise	8.5×10^{-15}
Detector noise	3×10^{-14}
LO phase noise	1.1×10^{-13}
Laser AM noise	2.8×10^{-13}
Laser FM-AM noise	1.7×10^{-13}
Total $\sigma_y(1s) = \sqrt{\sum \sigma_y^2}$	3.02×10^{-13}

3.5 Resume of the results achieved in the Mclocks project

The research undertaken under the Mclocks project allowed to reach important scientific and technological results. The main ones are listed in the following:

- The main results of the project were disseminated on a peer review journals: we published 14 papers in important research journal including: Physical Review A, Journal of Applied Physics, Applied Physics Letters, Review of Scientific Instruments, etc.
- The results of this research have been reported to important international congresses (like EFTF, IFCS), workshop, meetings etc., in the form of talk or poster.
- Three vapour-cell clocks addressing different industrial applications have been devised and developed.



- Thanks to a joint effort, now three NMIs (INRIM, OBSPARIS and UFC) are equipped with a ultra-low phase noise synthesis chain used to interrogate the atoms.
- In the perspective of a space application, the POP has been successfully demonstrated locking the laser frequency to the clock cell, without losing significantly in frequency stability performances.
- INRIM is undertaking a technological transfer to Leonardo Company for the realization of a Engineering Model of the POP clock for space applications. The project is funded by ESA under a GSTP programme: GSTP6.2 AO7935: Rubidium POP (co-funded by Leonardo Company).
- The POP clock has been included in the Near-Term Candidates for Future GPS Deployment in the Aerospace document AEROSPACE REPORT NO. TOR-2015-03893 written by J. C. Camparo and T. U. Driskell.
- A system to easily tune the cavity of Rubiclock has been investigated and realized. It will be adopted in the clocks produced by Muquans (industrial unfunded partner).
- Rubiclock has been successfully tested in 0g conditions during 6 parabolic flights.
- The push-pull technique applied to CPT clock has been successfully demonstrated. More physical insight has been gained on CPT phenomenon.
- A company demonstrated interest for the industrial development of the CPT clock implemented at UFC.
- The results of this project have been reported to the project's stakeholder committee, clocks manufacturers, national and European space agencies, other research laboratories in the final workshop that took place at INRIM (Torino, Italy) on June 22nd 2016.
- This project went beyond the state of the art in several aspects. First of all, a vapour cell clock using cold atoms has been developed and fully characterized, including a test in 0g condition. The activity performed during the project contributed to the know-how of the clock and then to the realization of the commercial prototype developed by Muquans. The metrological developments achieved by the POP clock stimulated the interest of a company (Leonardo Finmeccanica) which is going to realize an innovative clock for space based on the POP technique. Even though the main goal of the project was technologically oriented, research was also carried out. In this regard, very efficient and innovative CPT scheme have been devised and tested.

4 Actual and potential impact

Dissemination of results

The project outputs have been shared widely with the metrology community and instrumentation and clock manufacturers; 26 papers or posters have been published and 14 papers have been published in peer-review journals. A website has been established to promote the activities of the project and it includes e-training lectures. There is a stakeholder area where presentations can be uploaded so that members can disseminate information about the project activity. A tutorial presentation on vapour cell clocks was presented at the European Frequency and Time Forum (EFTF 2014), and 8 works (oral and posters) were presented.

The project was also presented at the workshop "Atomic clocks for Industry" together with EMRP project (IND14) New generation of frequency standards for industry. The project has been also presented to three EURAMET meetings. Results from the project have been presented at the Joint Congress EFTF-IFCS (Denver, April 2015), IEEE Workshop on Metroaerospace (Benevento, Italy, June 2015), the International Astronautical Congress (Jerusalem, Israel, 2015), the 8th Symposium on Frequency Standards and Metrology (Potsdam, October 2015) and at the EFTF congress (York, April 2016).



Impact

The innovative techniques and/or solutions have been presented to European clock manufacturers and space agencies. Demonstrating the technology and commercial potential of the new technologies will promote their use by clock makers and industry. The results will be useful to many institutes or companies whose activity is related to accurate and stable time and frequency signals, including those wanting to have stable and high performing which are cheaper and more compact than at present.

The pulsed optically pumped clock developed in this project will provide frequency stability comparable to passive Hydrogen masers, but from an instrument with much reduced volume and power consumption, and potentially low price than existing solutions. In addition, the cold atom vapour-cell clock can provide excellent frequency accuracy as a potential replacement of today's commercial Cs beam atomic clocks.

Commercial impact

The sensor company Muquans will adopt the device developed in the project to tune the cavity in their commercial clocks more easily. Another company is starting a collaboration with UFC for the industrial development of a miniaturised CPT clock.

Partially exploiting the results of the project, INRIM is undertaking a technological transfer to Leonardo Company for the realisation of an Engineering Model of the POP clock for space applications. The project is funded by ESA under a GSTP programme: GSTP6.2 AO7935: Rubidium POP (co-funded by Leonardo Company).

Potential impact

The outcomes of this project may impact also on metrology, fundamental research and dissemination of the SI second. A wide range of key European industries, including navigation, telecommunication, defence and precision instruments producers may experience significant benefits from the results of the present work. One of the main goals is therefore to disseminate frequency standards technology and capabilities that are now mainly located in European NMI or research institutes, to stakeholder and end-users and European clock manufacturer companies.

5 Website address and contact details

The address of the project public website is <http://www.inrim.it/Mclocks/>.

Coordinator: Salvatore Micalizio, INRIM, Italy, s.micalizio@inrim.it

Work Package Leaders:

- Stephane Guérandel, OBSPARIS, France, stephane.guerandel@obspm.fr
- David Holleville, OBSPARIS, France, david.holleville@obspm.fr
- Ersoy Sahin, TUBITAK, Turkey, ersoy.sahin@tubitak.gov.tr
- Rodolphe Boudot, UFC Femto-St, rodolphe.boudot@femto-st.fr

REG Researcher: Gaetano Mileti, Université de Neuchate, gaetano.mileti@unine.ch

6 List of publications

E.Sahin, G.Ozen, R.Hamid, M.Celik and A.Ch. Izmailov, Coherent Population Trapping resonances on lower atomic levels of Doppler broadened optical lines *Quantum Electronics Journal*, vol. 44 (Issue11) 1071–1076 (2014).

B. Francois, R. Boudot, J. M. Danet and C. E. Calosso, A low phase noise microwave frequency synthesis for a high-performance Cs vapor cell CPT atomic clock, *Rev. Sci. Instrum.* Vol. 85, 094709 (2014).

C. E. Calosso et al. Doppler-stabilized fiber link with 6 dB noise improvement below the classical limit, *Optics Letters*, Vol. 40, 131 (2015).

A. Godone, F. Levi, C. Calosso, and S. Micalizio, High performing vapor cell frequency standards, *Rivista del Nuovo Cimento* Vol. 38, 133 (2015).



S. Kang, M. Gharavipour, C. Affolderbach, F. Gruet, and G. Mileti, Demonstration of a high-performance pulsed optically pumped Rb clock based on a compact magnetron-type microwave cavity, *J. Appl. Phys.* Vol. 117, 104510 (2015).

Peter Yun, Jean-Marie Danet, David Holleville, Emeric de Clercq and Stéphane Guérandel, Constructive polarization modulation for coherent population trapping clock, *Appl. Phys. Lett.* Vol. 105, 231106 (2014).

B. François, C. E. Calosso, M. Abdel Hafiz, S. Micalizio and R. Boudot, Simple-design ultra-low phase noise microwave frequency synthesizers for high-performing Cs and Rb vapor-cell atomic clocks, *Rev. Sci. Instrum.* Vol. 86, 094707 (2014).

C. Affolderbach et al. Imaging Microwave and DC Magnetic Fields in a Vapor-Cell Rb Atomic Clock, *IEEE Trans. Instrum. Meas.* Vol. 64, 3629 (2015).

M. Abdel Hafiz and R. Boudot A coherent population trapping Cs vapor cell atomic clock based on push-pull optical pumping, *J. Appl. Phys.* Vol. 118, 124903 (2015).

S. Kang, M. Gharavipour, C. Affolderbach and G. Mileti, Stability limitations from optical detection in Ramsey-type vapour-cell atomic clocks, *Electron. Lett.* Vol. 51, 1767 (2015).

F. Levi, J. Camparo, B. François, C. E. Calosso, S. Micalizio, and A. Godone, Precision test of the AC-Stark shift in a vapor phase system, *Phys. Rev. A* Vol. 93, 023433 (2016).

G. A. Costanzo, S. Micalizio, A. Godone, J. C. Camparo, and F. Levi, ac Stark shift measurements of the clock transition in cold Cs atoms: Scalar and tensor light shifts of the D2 transition, *Phys. Rev. A* Vol. 93, 063404 (2016).

M. Hafiz, G. Coget, E. de Clercq, and R. Boudot, Doppler-free spectroscopy on Cs D 1 line with a dual-frequency laser, *Optics Letters* Vol. 41(13) 2982-2985 (2016).

P. Yun, F. Tricot, C. E. Calosso, S. Micalizio, B. François, R. Boudot, S. Guérandel, and E. de Clercq, High-Performance Coherent Population Trapping Clock with Polarization Modulation, *Phys. Rev. Applied* vol.7, 014018 (2017).

A.C. Cardenas-Olaya, E. Rubiola, J.-M. Friedt, P.-Y. Bourgeois, M. Ortolano, S. Micalizio, and C.E. Calosso, Noise Characterization of Analog to Digital Converters for Amplitude and Phase Noise Measurements, accepted on Review of Scientific Instruments, 2017.